Peer-reviewed version available at *Scientifics Reports* **2019**, *9*; doi:10.1038/s41598-019-54205-y

Article

Extraction of Polyphenols and Synthesis of New Activated Carbon from Spent Coffee Grounds

Marina Ramón Gonçalves [1], Lorena Alcaraz[1], Susana Pérez-Ferreras [2], María Eugenia León-González[3], Noelia Rosales-Conrado[3] and Félix A. López [1,*]

[1] Centro Nacional de Investigaciones Metalúrgicas (CENIM). Consejo Superior de Investigaciones Científicas (CSIC). Avda. Gregorio del Amo, 8. 28040 Madrid, Spain. marina@cenim.csic.es; alcaraz@cenim.csic.es; f.lopez@csic.es

[2] Instituto de Catálisis y Petroleoquímica (ICP). Consejo Superior de Investigaciones Científicas (CSIC). C/ Marie Curie, 2. 28049 Madrid, Spain; spferreras@icp.csic.es

[3] Departamento de Química Analítica. Facultad de Ciencias Químicas. Universidad Complutense de Madrid, 28040 Madrid, Spain. leongon@quim.ucm.es; noerosales@quim.ucm.es

* Correspondence: f.lopez@csic.es

Abstract: A valorization process of spent coffee grounds (SCG) was studied. Thus, a two-stage process, a stage of extraction of the polyphenols and a stage of obtaining activated carbon (AC) by a carbonization process, was performed. The extraction was carried out with a hydro-alcoholic solution in a pressure reactor, modifying time and temperature. To optimize the extraction of polyphenols, a two-level factorial design with three replications at the central values was used. The best results were obtained by performing the extraction at 80 °C during 30 min, using a mixture of EtOH:H_2O 1:1 (v/v) as extraction solution. Caffeine and chlorogenic acid were the most abundant compounds in the analyzed extracts, ranging from 0.09 to 4.8 $mg \cdot g^{-1}$ and 0.06 to 9.7 $mg \cdot g^{-1}$, respectively. The precursor obtained in the extraction stage were transformed into AC. An experimental design was realized in order to analyze the influence of different variables in the AC obtained process (reaction time and amount of potassium hydroxide used). Actived carbons with BET specific surface (S_{BET}) comprised between 1600 $m^2 \cdot g^{-1}$ and 2330 $m^2 \cdot g^{-1}$ had a microporous surface. Under the optimum conditions, the obtained AC presented a maximum adsorption capacity of methylene blue (q_m) between 411 $mg \cdot g^{-1}$ and 813 $mg \cdot g^{-1}$.

Keywords: spent coffee grounds; polyphenols; extraction; subcritical fluid; activated carbon; methylene blue; adsorption.

1. Introduction

Coffee is a popular and consumed beverage worldwide and during the last 150 years has grown steadily in commercial importance [1–6]. As reported by the International Coffee Organization (ICO, 2017), coffee production suffered significant increased in recent years [7,8] and large amounts of coffee waste such as pulp, husk and coffee beans are generated daily.

In the upcoming years, with the high coffee production and the concern about waste management [1,4], it is necessary to find novel applications for reusing coffee residues. These residues contain substantial amounts of high value-added products for example carbohydrates, proteins, pectins and bioactive compounds as polyphenols, which could be extracted and employed in the cosmetic, pharmaceutical and food industries [4,9]. So, one of them could be the efficient extraction of polyphenols and the production of different value-added compounds, leading to better management of these wastes and to reduce the environmental impact that they generate, such as the generation of greenhouse gases [4,10,11]. There are numerous studies focused on the extraction of bioactive compounds from different food by-products. Other applications for spent coffee grounds (SCG) are antioxidants, anti-inflammatory additives, for the production of biofuels, as a complement in animal feed or, fertilizers [2,4,11,12].

The polyphenols present in SCG are an group of secondary metabolites of plants, which are the constituents of a great number of fruit and vegetables, and beverages such as tea, coffee and wine and the main antioxidants in the human diet [13]. Caffeic acid is a well-known non-flavonoid phenolic compound abundant in coffee, presenting potent antioxidant and neuroprotective properties [14]. Polyphenols might have different properties as an antioxidant, antiproliferative, anti-allergic, anticarcinogen, antimicrobial, antitumor, anti-inflammatory and neuroprotective activities [7,15], that are of potential attention for the agrifood, cosmetic and pharmaceutical industries [4,16,17].

Otherwise, AC is a porous solid with adsorbent and catalytic properties that is used in many industrial sectors. Their textural properties, including their high specific surface and microporosity, makes it an ideal compound to eliminate contaminants through physical adsorption processes [18]. Commercial ACs are mostly obtained from biomass waste [19,20]. Besides, many researches have been developed on the employ of biomass as a precursor of carbon active such as residues derives form tea, coffee or grapes and olives bones [6,21,22]. Within its wide variety of applications, the most common is the use of AC to removal several pollutants from wastewater due to its simplicity and low cost [9,18,23–25]. Other applications are the employment as a decolourizer for food industry, catalysis, purification of the chemical and pharmaceutical industry, for the elimination of gases, improving the noble metals or storing energy [26,27].

For all these reasons, the aim of the present work was the reuse and valorization of spent coffee grounds by the recovery, identification and quantification of bioactive polyphenols followed by synthesis of active carbon with high specific surface area. Thus, spent coffee grounds were previously subjected to a hydro-alcoholic extraction process under subcritical conditions to obtain an extract that contains the bioactive compounds and a solid (precursor). Next, the extract containing polyphenols was subjected to an evaporation process at low pressure, which allowed recovering the alcohol and reuses it in the extraction stage, and an aqueous solution in which the polyphenols were concentrated. Finally, the precursor was turned into AC by chemical activation and their morphological and textural properties were studied. Methylene blue (MB) adsorption capacity in solution was studied in the AC that presented the best textural properties. Figure 1 schematically describes the process studied.

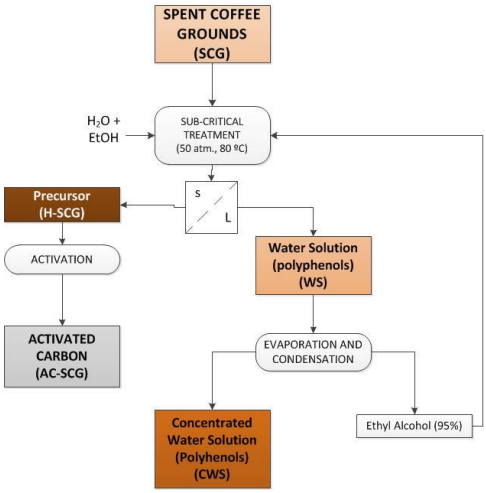

Figure 1. Scheme of the process studied

2. Results and Discussion

2.1. Optimization of polyphenol extraction conditions by experimental design

For optimization of the conditions for the extraction of polyphenols from spent coffee ground (SCG) a total of 11 runs were performed (Table S1). Analysis of the experimental results allowed determining the most favorable experimental extraction conditions for the maximum response. The values obtained from the extraction process are shown in Table S2. Experiment Nº. 6 showed higher extracted amounts (mg·g^{-1}) for caffeine, caffeic acid and trans-ferulic acid, while for rutin and naringin the conditions of experiment Nº. 8 provided higher contents. For resveratrol, a similar extracted amount was obtained in all the experiments, whereas in the case of kaempferol, it was below its limit of quantification (LOQ) determined by cLC-DAD.

The experimental factors were related with responses using a first-order polynomial model according to Equation (1):

$$\text{Response} = \beta_0 + \beta_1 T + \beta_2 t + \beta_3 E + \beta_{12} Tt + \beta_{13} TE + \beta_{23} tE \quad (1)$$

where β_0 is the intercept, β_1-β_3 are the temperature (T), time (t) and proportion of extraction solvent (E) linear coefficients, respectively, and β_{12}, β_{13}, and β_{23} are the interaction coefficients of the described above experimental factors. Amount extraction (mg·g^{-1}) of caffeine and polyphenols studied were fixed as responses. The parameter values that fit experimental data into Equation (1) for each of the analyzed analyte, as well as the statistic p-values are shown in Table S3. As can be observed, very disparate, positive and negative equation coefficients were obtained for each analyzed polyphenol, which means that the influence of the studied factors is markedly different. Negative values imply that the response decreased with the increased of the specified factor, while positive ones produced the contrary effect. In addition, the higher the value of an equation coefficient is, the more influence on the response it has. The results obtained show, in general, low significant effects for the studied factors, although both the temperature and extraction solvent were the most important factors affecting the response. Moreover, the obtained correlation coefficients (R^2) between 0.667 and 0.999 were achieved.

In order to determine the most significant effects and their interactions on the studied responses, estimated normalized response surfaces for each analyte were plotted. As an example, Figure 2 shows the three-dimensional graphs obtained for cafeic acid and rutin in the extracts obtained from spent coffee ground sample (WS). As can be seen, the amount of caffeic acid in the extraction solution increased with the ethanol ratio in the extraction solvent and the extraction time, while the concentration of rutin was more influenced by both extraction time and temperature. The data included in Table S3 agreed with all response surfaces.

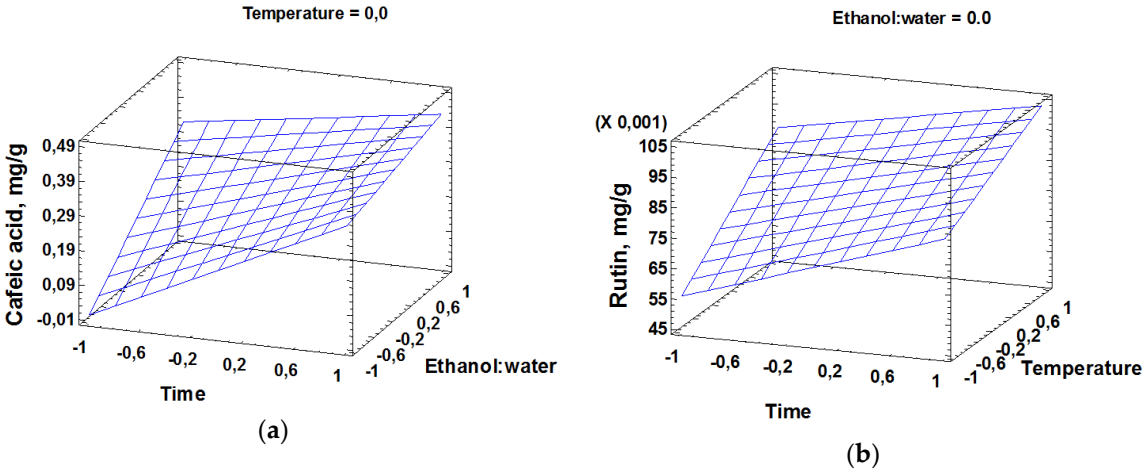

Figure 2. Estimated normalized response surfaces obtained for the content (mg·g^{-1}) of cafeic acid (a) and rutin (b) extracted from spent coffee ground sample (WS), both at different extraction times and ethanol:water mixtures or temperatures. Temperature was fixed at 100 ºC (a), ethanol:water ratio at 35:65 (v/v) (b).

Because of the experimental extraction conditions that provided the maximum responses depending on the analyte, multiple response analysis (MRA) was made. In this way, it is possible determine the combination of the experimental factors which simultaneously optimized the studied responses. So, the desirability function is maximized. As a compromise, the optimum conditions to obtain the maximum responses for the target analytes were 30 min of the extraction time, a temperature of 80 °C, a mixture of EtOH:H_2O (1:1, v/v) as extraction solvent, and an extraction pressure of 50 bar. Under these conditions, experimental responses were in agreement with those predicted by means of the experimental design analysis.

2.2. Polyphenols determination by cLC-DAD in the extracts from SCG

Individual polyphenols determination in the extracts obtained from SCG, in the extracts from precursor (H-SCG), in the extracts obtained before the evaporation process and the solutions obtained after the evaporation process (the aqueous solution in which the polyphenols are concentrated (CWS) and the organic solution (ethanol)), were performed by cLC-DAD. The chromatogram of the mixture of the standards used for the identification of the different polyphenols studied is shown in Figure 3. Table 1 shows the extracted amount of each analyte in mg per gram of dried sample in the distinct extracts evaluated. As can be observed, CWS presented the highest content of polyphenols and caffeine (except rutin and kaempferol) followed by SCG, while the other extract (WS, H-SCG and ethanol) were found at lower amounts. In addition, it is observed that the evaporation process allows to concentrate polyphenol and caffeine compounds in an aqueous solution, while residual amounts remain in the organic solution.

Table 1. Phenolic compounds and caffeine extracted from different solutions.

Compound (mg g^{-1})/ Sample Code[1]	**SCG**	**H-SCG**	**WS**	**CWS**	**Ethanol**
Caffeine	2.48	0.26	0.99	4.83	0.09
Chlorogenic acid	LOD	LOD	n.d	9.69	LOD
p-Coumaric acid	0.16	0.23	n.d	0.35	0.05
trans-Ferulic acid	0.17	0.16	0.11	0.18	0.02
Rutin	0.09	LOD	0.06	LOD	LOD
Naringin	0.21	0.10	0.14	0.42	0.01
Resveratrol	0.07	0.07	0.07	0.09	0.01
Quercetin	0.08	0.07	n.d	0.10	0.02
Kaempferol	0.05	0.10	LOD	0.03	0.01

[1] Extracted amounts are expressed as mg per gram of dried sample. LOD: determined at the levels of the method detection limit, n.d: no detected, SCG = extract from spent coffee grounds, H-SCG = extract from precursor, WS = extract obtained before the evaporation process, CWS = concentrated extract obtained after the evaporation process, Ethanol = organic solution obtained after the evaporation process.

Preprints (www.preprints.org) | NOT PEER-REVIEWED | Posted: 20 September 2019 doi:10.20944/preprints201908.0093.v2

Peer-reviewed version available at Scientifics Reports 2019, 9; doi:10.1038/s41598-019-54205-y

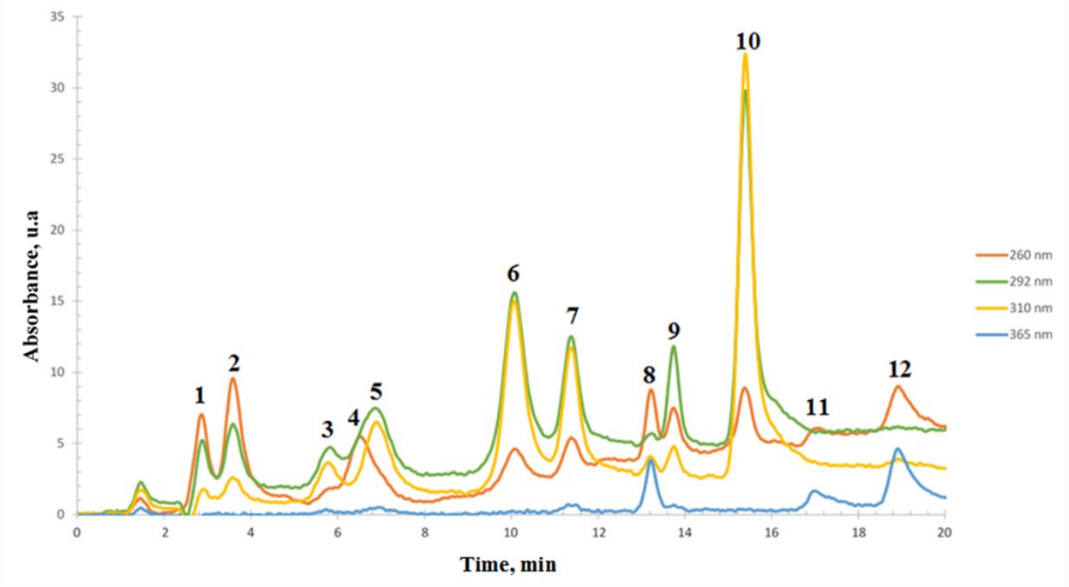

Figure 3. Chromatogram of the standard mixture (80 µg/L) obtained using the cLC-DAD optimized method. 1 (Gallic acid, t_R = 3.1 min, $\lambda_{óptima}$ = 292 nm); 2 (Dihydroxybenzoic acid, t_R = 4.0 min, $\lambda_{óptima}$ = 260 nm); 3 (Chlorogenic acid, t_R = 6.4 min, $\lambda_{óptima}$ = 310 nm); 4 (Caffeine, t_R = 7.2 min, $\lambda_{óptima}$ = 260 nm); 5 (Caffeic acid, t_R = 8.2 min, $\lambda_{óptima}$ = 310 nm); 6 (p-Coumaric acid, t_R = 11.1 min, $\lambda_{óptima}$ = 310 nm); 7 (Trans- Ferulic acid, t_R = 12.2 min, $\lambda_{óptima}$ = 310 nm); 8 (Rutin, t_R = 13.6 min, $\lambda_{óptima}$ = 260 nm); 9 (Naringin, t_R = 14.4 min, $\lambda_{óptima}$ = 292 nm); 10 (Resveratrol, t_R = 16.2 min, $\lambda_{óptima}$ = 310 nm); 11 (Quercetin, t_R = 17.6 min, $\lambda_{óptima}$ = 260 nm); 12 (Kaempferol, t_R = 19.7 min, $\lambda_{óptima}$ = 365 nm).

2.3. Estimation of total flavonoid (TFC) and total polyphenol content (TPC), and total antioxidant capacity (TAA) in the extracts obtained from SCG

TFC, TPC and TAA of the obtained extracts from SCF under optimum extractions conditions were evaluated. The results obtained in the spectrophotometric methods for WS and CWS were 14 ± 8 mg GAE·g^{-1} DW for TPC, 10.7 ± 0.8 mg QE·g^{-1} DW for TFC, 14.5 ± 0.3 mg GAE·g^{-1} DW for TAA, and 49 ± 1 mg GAE·g^{-1} DW for TPC, 56 ± 7 mg QE·g^{-1} DW for TFC and 23 ± 2 mg GAE·g^{-1} DW for TAA, respectively. As can be observed, after the evaporation process, there was an increase in the TFC and TPC and TAA in the extract obtained.

2.4. Optimization of textural and morphological properties by factorial experimental design and characterization of active carbon

For optimization of the textural and morphological properties of AC from precursor (H-SCG) under the optimal conditions, a factorial experimental design was made. Once a total of 11 experiments were performed, analysis of the experimental results permitted determining the most favorable obtaining conditions for the maximum response. The experimental factors were related with responses using a first-order polynomial model according to Equation (1). The parameter values that fit experimental data into Equation (1) for each of the analyzed analyte are shown in Table S4. The results obtained for S_{mi}, S_e and S_{BET} show significant effects for time and temperature factors, and for interaction factors such as temperature and KOH:precursor. Furthermore, the obtained correlation coefficients (R^2) between 0.798 and 0.985 were achieved. Table S5 shows the textural properties of the ACs obtained in the experiment performed by experimental design. As can be observed, the ACs have a microporous microstructure ($S_{mi} \approx S_{BET}$), their volume of micropores (W_o) is similar to the pore volume (V_p). The pore sizes (L_o) are, in all cases, less than 2 nm. The BET surface area varies between 1377-2330 m^2·g^{-1}. The nitrogen adsorption isotherms carried out at -196 °C for the ACs of the experiments No. 3 and 5 that correspond to those that have the highest and lowest specific surface of all the active carbons obtained are shown in Figure 4. According to the International Union of Pure and Applied Chemistry (IUPAC), the shapes of the isotherms are of type I and II. At low

relative pressures ($p/p_0 < 0.1$), large volumes of N_2 were adsorbed for both samples [28]. The quantity adsorbed of N_2 at $p/p_0 \sim 1$ varies between 350 and 758 $cm^3 \cdot g^{-1}$.

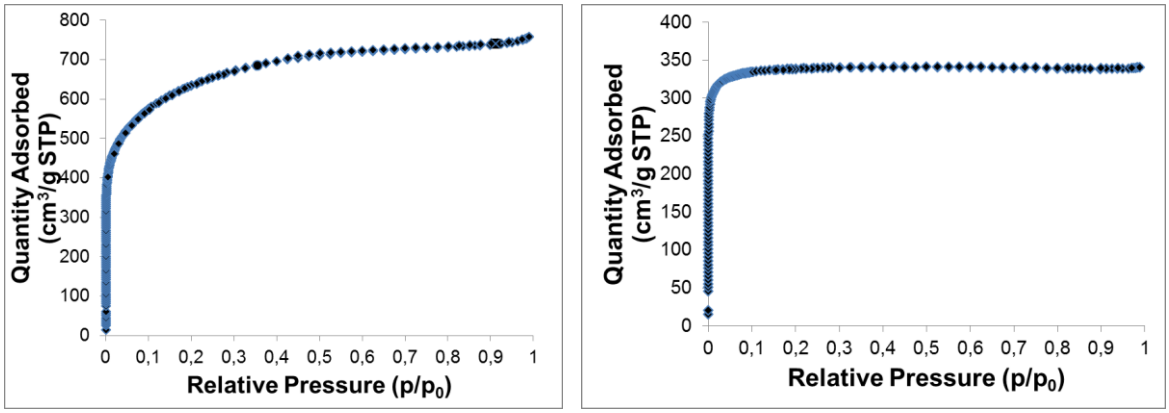

Figure 4. N_2 adsorption isotherms at 77 K for the activated carbons of the experiments No. 3 (a) and No. 5 (b).

As in the case of the extraction of polyphenols, estimated normalized response surfaces were plotted for the studied responses. Figure 5 shows the three-dimensional graphs obtained for S_{BET} and W_o in the sample studied. The rest of responses present surfaces similar to those shown in Figure 5, where the response variable increases with the temperature. The data included in Table S4 agreed with all response surfaces

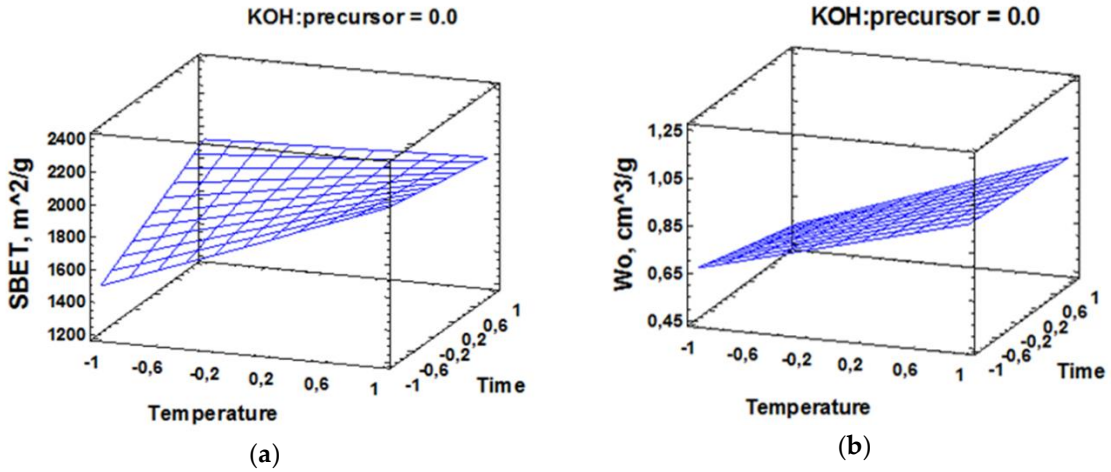

Figure 5. Estimated normalized response surfaces obtained for the S_{BET} (a) and W_o (b) from optimized active carbon (AC-SCG), both at different times and temperatures. KOH:precursor was fixed at 2:1 (m/m).

Moreover, it was necessary to carry out MRA due to the heterogeneity in the experimental conditions. As a compromise, the optimum conditions to obtain the maximum responses were a time of 1 h, a temperature of 850 °C, and a mixture of KOH:precursor at the ratio 2.5:1. Under these conditions, the experimental responses were in agreement with those predicted by means of the experimental design analysis.

Table 2 shows the variation of the burn-off and yield of the activation process in the assays carried out in the experimental design. As the carbonization temperature increases, the burn-off increases and the recovery in weight of the AC decreases. The burn-off values vary between 82 % and 96 % and the yields between 4 % and 18.5 %. Table 3 compares the elemental chemical compositions of the initial residue, precursor and AC. It can be verified that the C content has increased up to 84 % in AC as a consequence of the carbonization process used.

Table 2. The variation of the burn-off and yield of the activation process.

Experiment	Burn-off (wt, % daf[1])	Yield (wt, %)
AC-SCG-1	82.0	18.0
AC-SCG-2	82.0	18.0
AC-SCG-3	95.0	5.0
AC-SCG-4	96.0	4.0
AC-SCG-5	81.5	18.5
AC-SCG-6	86.5	13.5
AC-SCG-7	93.0	7.0
AC-SCG-8	96.0	4.0
AC-SCG-9	88.7	12.0

[1] daf: dry ash-free basis

Table 3. Elemental composition (ultimate analysis) of the spent coffee grounds and activated carbon

	SCG	H-SCG	AC-SCG-8
Ultimate analysis			
C (wt, % daf)	51.19	51.58	83.89
H (wt, % daf)	6.43	6.82	1.13
N (wt, % daf)	2.58	2.06	0.45
S (wt, % daf)	0.11	0.08	0.12
O[1] (wt, % daf)	39.77	39.46	15.24

[1] By subtration

Finally, Figure 6 shows the morphology of several ACs examined by FE-SEM in which the microporous nature of the carbons can be appreciated. As can be observed, the AC from experiment 3 has a greater number of pores than that of experiment 5.

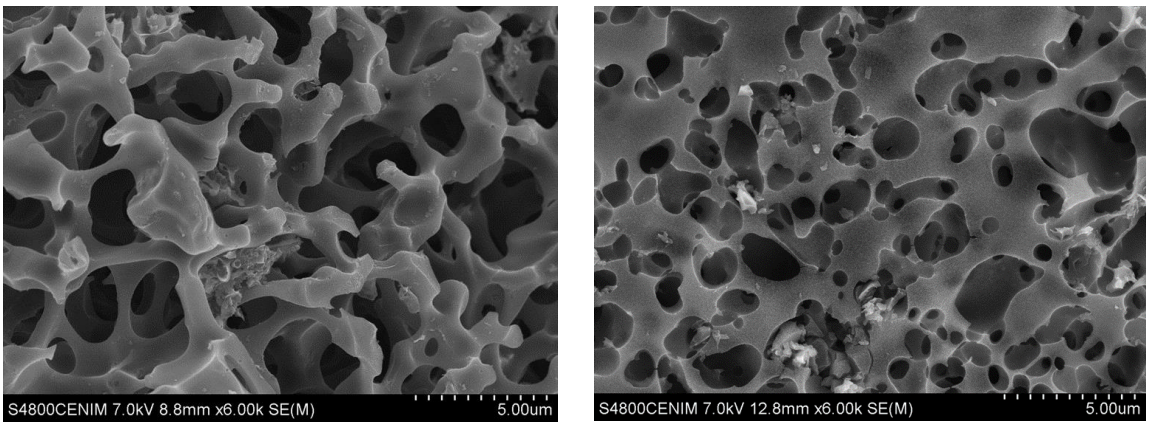

(**a**) (**b**)

Figure 6. Morphology of active carbons from experiment 5 (a) and experiment 3 (b) examined by FE-SEM.

2.5. Adsorption of methylene blue

2.5.1. Thermodynamic adsorption studies

In order to analyze the possible MB adsorption mechanism different isotherms were assessed at different temperatures. The calculated parameters values for the different isotherms in the linear form, using the Equations 5-7, are summarized in Table 4.

Preprints (www.preprints.org) | NOT PEER-REVIEWED | Posted: 20 September 2019 doi:10.20944/preprints201908.0093.v2

Peer-reviewed version available at Scientifics Reports 2019, 9; doi:10.1038/s41598-019-54205-y

Table 4. Langmuir, Freundlich and Temkin parameters calculated for MB adsorption.

		T (°C)		
		30	60	80
Langmuir	q_m (mg g^{-1})	411.5	775.2	813.1
	B (mg^{-1})	18.7	8.9	3.7
	R_L	0.003	0.006	0.013
	R^2	0.999	0.999	0.993
Freundlich	K_f (g^{-1})	340.8	567.2	510.9
	n	6.4	3.6	3.9
	1/n	0.2	0.3	0.3
	R^2	0.972	0.819	0.988
Temkin	A_t	4011.9	224.5	400.3
	b_T	60.3	24.9	31.5
	R^2	0.962	0.921	0.905

The highest obtained R^2 correlation coefficient values were for the Langmuir isotherm, which are displayed in Figure 7 each of the studied temperature.

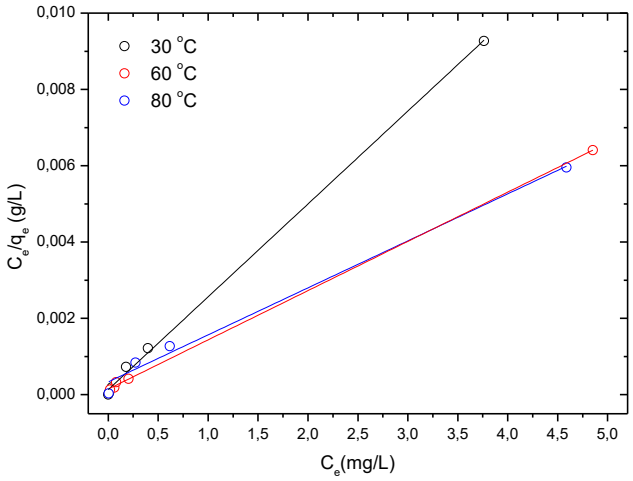

Figure 7. Langmuir isotherm at different temperatures.

The calculated values q_m increase with the temperature, in accordance to previous studies related to the MB adsorption by ACs obtained from different wastes [29,30]. In addition, the calculated values are similar to the q_m experimental obtained (between 411-813 $mg \cdot g^{-1}$).

The calculated Langmuir non-dimensional factor (R_L) in all cases were between the range of $0<R_L<1$. These results reveal that the adsorption is a favorable process [31] independently of the temperature of the adsorption experiment.

Thermodynamic parameters were calculated at different temperatures using Equations (11)-(12). The negative value obtained of enthalpy (ΔH^0) (-77.81 $J \cdot mol^{-1}$) indicates that the process is exothermic. In addition, the entropy (ΔS^0) was positive, 68.10 $J \cdot mol^{-1} \cdot K^{-1}$, which indicate the increased disorder at the solid solution interface components. Finally, the free Gibbs energies (ΔG^0) (-205.73 $kJ \cdot mol^{-1}$ at 30 °C; -226.17 $kJ \cdot mol^{-1}$ at 60 °C and 239.79 $kJ \cdot mol^{-1}$ at 80 °C) were also negatives and exhibit that this process is spontaneous and favorable thermodynamically.

Preprints (www.preprints.org) | NOT PEER-REVIEWED | Posted: 20 September 2019 doi:10.20944/preprints201908.0093.v2

Peer-reviewed version available at Scientifics Reports 2019, 9; doi:10.1038/s41598-019-54205-y

2.5.2. Kinetic adsorption studies

The adsorption kinetics experiments of MB were also performed at different temperatures. Table 5 exhibits the obtained results.

Table 5. Kinetic parameters and correlation coefficients for the MB adsorption.

T (°C)	Pseudo-first order			Pseudo-second order		
	k_1 (min^{-1})	q_e (mg g^{-1})	R^2	k_2 (g min mg^{-1})	q_e (mg g^{-1})	R^2
30	0.046	38.05	0.871	2.85 10^{-3}	201.99	0.999
60	0.097	92.5	0.965	3.77 10^{-3}	200.49	0.999
80	0.101	36.73	0.877	7.60 10^{-3}	199.74	0.999

Figure 8 exhibits a pseudo-second-order model was the best fit in all cases, such as indicated the correlation coefficients obtained. K_2 constant values calculated at different temperatures (2.85·10^{-3} g·min·mg^{-1}, 3.77 g·min·mg^{-1} and 7.60 g·min·mg^{-1} for 30 °C, 60 °C and 80 °C, respectively) increased with temperature, which indicate an enhance of the MB adsorption. The process activation energy (E_a) was calculated fitting the observed kinetics rate constants logarithm ($\ln K_{2,obs}$) versus the inverse of temperature (1/T) (Figure 8), where the slope is $-E_a/R$ [32]. This value is used to estimate whether the process is a physical (readily reversible reactions and the energy requirements are small between the range of 5 to 40 kJ·mol^{-1} or chemical adsorption (process that requires higher energies, between 40 to 800 kJ·mol^{-1}, with stronger forces) [32]. The calculated activation energy in the present case was 77.86 kJ·mol^{-1}. The obtained value suggested a chemisorption process.

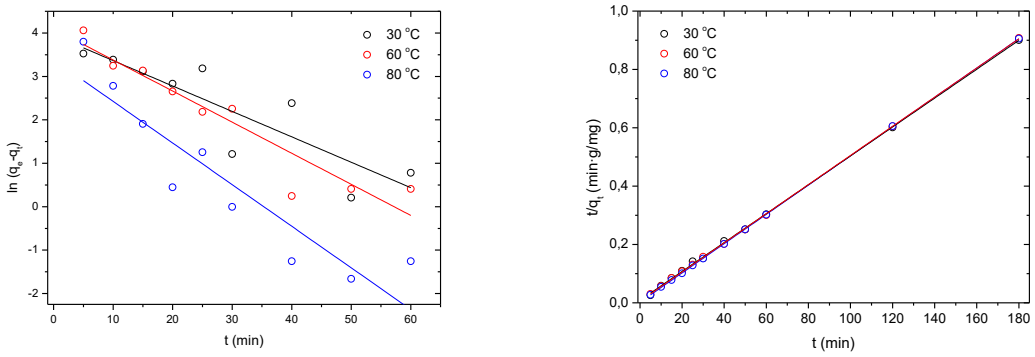

(**a**) (**b**)

Figure 8. Pseudo-first (a) and pseudo-second (b) kinetics for MB adsorption at different temperatures.

Isothermal and kinetic models, q_m and the activation agent of various adsorbents are exhibit in Table 6. As can be observed, many cases the KOH is used as an activation agent. In general, a better fit to the Langmuir model were found for the adsorption isotherms. Moreover, the adsorption kinetics fitted a pseudo-second-order model in the majority of the presented cases. In relation to the capacity of adsorption, the spent coffee ground has a wide range together with the residues of the carpets, while the rest of the intervals are smaller. Finally, in the case of the unique values, the q_m presents a value around 400 mg·g^{-1}, with some exception as in the orange peel, wine wastes.

Table 6. Maximum monolayer adsorption capacity, isothermal and kinetic models of various adsorbents for MB.

Precursor of activated carbon	Activation agent	Maximum monolayer adsorption capacity (q_m mg g^{-1})	Isothermal model	Kinetic model	References
Spent coffee grounds[1]	KOH	411-813	Langmuir	Pseudo-second order	This work
Wine wastes[1]	KOH	714-847	Langmuir	Pseudo-second order	[29]
Wastes carpets	H_3PO_4	403-769.2	Langmuir	Pseudo-second order	[33]
Date stones	$ZnCl_2$	398.2	Langmuir	Pseudo-second order	[34]
Bamboo	KOH	454.2	Langmuir	Pseudo-second order	[35]
Coconut husk	KOH	437.8	Langmuir	Pseudo-second order	[35]
Vetiver roots	H_3PO_4	423	Langmuir	Pseudo-second order	[36]
Acorn shell	$ZnCl_2$	312.5	Langmuir	-	
Sucrose[1]	KOH	704.2	Langmuir	Elovich	[37]
Hazelnut shells[1]	KOH	524.0	Langmuir	Pseudo-second order	[26]
Posidonia oceanica (L.)	$ZnCl_2$	285.7	Langmuir	Dubinin-Raduchkevich	[38]
Orange peel	$ZnCl_2$	150.0	-	-	[39]
Peach Stones	H_3PO_4	444.3	Tóth and Redlich Peterson	-	[40]
Grape waste	$ZnCl_2$	417.0	Langmuir	-	[41]
Waste tea	CH_3COOK	554.3	Langmuir	-	[42]
Phoenix dactylifera fruit pits	NaOH and KOH	104-146	Langmuir	Pseudo-second order	[43–45]

[1] Hydrothermal treatment for obtained the precursor

3. Materials and Methods

3.1. Obtaining the SCG

The waste recovered after coffee beverage preparation (SCG, spent coffee ground) comes from the canteen of the National Center for Metallurgical Research (Superior Council of Scientific Investigations) in Madrid. The coffee used was a mixture 10 (wt,%) roasted and 90 (wt,%) natural roasted (obtained at 9 bar and 88 °C). The sample was maintained at -20 °C until analysis. Moisture content of spent coffee ground was obtained by drying at 80 °C during 48 h.

3.2. Capillary LC-DAD and spectrophotometric analysis

An Agilent cLC instrument Mod. 1100 Series (Agilent Technologies, Madrid, Spain) formed by a G1379A degasser, a G1376A binary capillary pump and a G1315B diode array detector (500 nL, 10 mm pathlength) was used for cLC analysis. A stainless steel loop with a volume of 10 µL was coupled to a Rheodyne® injection valve. The capillary analytical column was a Synergy TM Fusion 4 µm C18 (150 mm x 0.3 mm I.D.) from Phenomenex (Torrance, CA, USA). Data acquisition and processing were performed with the Agilent Chemstation software package for Microsoft Windows.

The chromatographic method (cLC-DAD) developed by León-González et al., 2018 [46] was employed for caffeine and polyphenols identification. The wavelengths 220, 260, 292, 310 and 365 nm were chosen for the UV-diode array detection. Quantitative analysis was made at 260 nm for 3,4-dihydroxybenzoic, caffeine, rutin and quercetin, 292 nm for both naringin and gallic acid, 310 nm for chlorogenic acid, trans-ferulic acid resveratrol and p-coumaric acid and 365 nm for kaempferol. For focusing purposes, injections were made in an aqueous solution containing 1 % (v) of ACN and 0.1 % (v) TFA pH 3.24.

The spectrophotometric methods described by Vijayalaxmi et al., 2015 y Shrikanta et al.,2015 [12,47] with some changes were employed for determining TFC, TPC and TAA.

3.3. Optimization of polyphenols extraction conditions by experimental design

The extraction of polyphenols from SCG were done in a Berghof BR3000 reactor at controlled temperature and pressure. An amount of 45 g of SCG were added to 600 mL of a hydro-alcoholic solution with different ratios of ethanol (EtOH) (Table S1). The extraction time was varied between 15 and 30 min, and the extraction temperature in the range 80-120 °C. The pressure was kept constant at 50 bar. Once completed the extraction process, the reactor was cooled and the resulting suspension was centrifuged for 1 h. The solid obtained (H-SCG) was separated, and an aliquot of the resulting solution was used to quantify the individual polyphenol and caffeine present in the sample by cLC-DAD.

On the other hand, a two-level factorial design with three replicates at the center point was planned to maximize the extracted amount of the target polyphenols and caffeine from SCG samples. A previous chromatographic study was carried out for identification of the experimental factors that could most influence the polyphenol extraction: extraction time, extraction temperature, pressure and nature of the extraction solution. As result, nature of the extraction solution, extraction time and extraction temperature were selected as experimental factors and included in the experimental design. Experimental levels of the selected factors are included in Table S1. Amount extraction ($mg \cdot g^{-1}$) of caffeic acid, rutin, trans-ferulic acid, naringin, kaempferol, resveratrol and caffeine were fixed as responses, and the optimization criterion for the analysis of the performed experimental design was the maximization of response values for the analytes evaluated.

Once the extraction process was optimized, the hydro-alcoholic solution obtained under optimum conditions, containing the maximum amounts of the polyphenols extracted (WS), was evaporated in a rotavapor R-100 (Buchi) at 110 mbar pressure and at a temperature of 40 °C, yielding a concentrated aqueous solution of polyphenols (CWS) and a fraction of ethyl alcohol, which could be reused in the extraction process.

3.4. Optimization by factorial experiemntal design and characterizacion of active carbon

The precursor obtained under optimum extraction conditions (experiment nº6, Table S1) was used to obtain AC by a method of chemical activation with KOH. Thus, 1 g of the carbonaceous precursor was mixed with different amounts of KOH, between 1.5 and 2.5 g. The resulting mixtures were homogenized with a ball mill, placed in alumina crucibles and treated in a Carbolite STF 15 tubular oven at 850 °C for a variable time between (30-60 min), under a nitrogen carrier ($150\ mL \cdot min^{-1}$). Later cooling to room temperature, the solid was washed with Milli-Q water until neutral pH. After that, it was dried in an oven at 80 °C for 12 h.

The degree of activation (burn-off) was determined using Equation (2):

$$\text{Burn-off (wt\% daf)} = \left({}^{w_1 - w_2}/_{w_1}\right) \times 100 \qquad (2)$$

where w_1 and w_2 are the mass (dry ash-free [daf] basis) of carbonaceous material before and after activation.

The yield of the activation process was determined by Equation (3):

$$\text{Yield (wt, \%)} = {}^{w_2}/_{w_1} \times 100 \qquad (3)$$

The porous structure of the AC was determined by nitrogen adsorption at -196 °C (77 K) sing the Micromeritics ASAP 2020. The samples were partially degassed at 350 °C (623 K) for 16 h. The specific surface area was computed using the adsorption isotherm via the BET equation and DFT models, using Micromeritics and Quantachrome software. The surface of ACs was examined by field emission scanning electron microscope (FE-SEM) using a Hitachi S 4800 J microscope.

For optimization of the textural and morphological properties of obtained AC, a two-level factorial design with three replicates at the center point was employed. Time, temperature and different amounts of KOH were selected as experimental factors. Experimental levels of the selected factors are included in Table S6. The total volume of pores (V_p), volume of micropores (W_o), the size of the micropores (L_o), the microporous surface (S_{mi}), the non-microporous external surface (S_e) and the specific surface area (S_{BET}) were chosen as responses, and the optimization criterion for the analysis of experimental design was maximization of the response values.

3.5. Batch adsoprtion experiements

The adsorption capacity of MB by the obtained AC was investigated. Different experiments adsorption were carried out. For it, 10 mg of the PCF-28 CA were added to MB solutions of concentration 10 mg·L^{-1}. The mixtures were magnetically stirred at 350 rpm in a thermostatic-controlled bath. Aliquots were extracted every 5 min (up to 30 min), every 10 min (up to 60 min) and finally, every 60 min (until equilibrium is reached). The amount of the MB in solution was calculated by UV-Vis spectroscopy at 610 nm employing a Zuzi spectrophotometer 4101.

The adsorbed MB amount per gram of AC (q_e) was calculated from Equation (4):

$$q_e = {(C_0 - C_e)V}/{m} \quad (4)$$

Where C_o and C_e are the initial and at the equilibrium MB concentration in the solution (mg·L^{-1}), respectively, V is the volume of the solution (L) and m is the mass of the AC (g) employed.

In order to evaluate the thermodynamic study, the linear form of the isotherms of Langmuir (Equation (5)), Freundlich (Equation (6)) and Temkin (Equation (7)) were employed and the AC amount were modify.

$${C_e}/{q_e} = {1}/{q_m b} + {1}/{q_m}\, C_e \quad (5) \quad [48]$$

$$ln\ q_e = ln\ K_F + 1/n\ ln\ c_e \quad (6) \quad [49]$$

$$q_e = B \cdot ln\ A_T + (RT/b_T) \cdot \ln c_e \quad (7) \quad [50]$$

where C_e and q_e are the MB concentration (mg·L^{-1}) and the MB amount adsorbed per mass of AC at equilibrium (mg·g^{-1}), respectively; q_m is the maximum adsorption capacity of the AC (mg·g^{-1}) and b is the Langmuir equilibrium constant (L·mg^{-1}); K_F (L·g^{-1}) and n are adsorption constants; AT is the Temkin isotherm equilibrium binding constant (L·g^{-1}), b_T is the Temkin isotherm constant and R is the universal gas constant (8.314·103 kJ·K^{-1}·mol^{-1}).

The non-dimensional Langmuir constant (R_L) was determined using the Equation (8):

$$R_L = 1/(1 + bC_0) \quad (8)\ [31]$$

Where C_0 is the initial concentration of MB (mg·L^{-1}).

So, the value of R_L determines if the process is unfavorable (R_L>1), linear (R_L=1), favorable (0<R_L<1) or irreversible (R_L=0) [51].

The kinetic data were evaluated employing a pseudo-first-order (Equation (9)) and pseudo-second-order models (Equation (10)) [52]:

$$ln\ (q_e - q_t) = ln\ q_e - K_1 t \quad (9)$$

$$t/q_t = 1/(K_2\, q_e^2) + 1/q_w\ t \quad (10)$$

where K_1 and K_2 are the pseudo-first (min^{-1}) and pseudo-second-order ($g \cdot mg^{-1} \cdot min$) adsorption constants.

Finally, the thermodynamic equilibrium constant as the Gibbs free energy (ΔG^0) (Equation (11)), the standard enthalpy (ΔH^0) and the entropy (ΔS^0) (Equation (12)) [53] were determined using:

$$\Delta G^0 = -RT \ ln \ K_a \quad (11)$$

$$ln \ K_a = \Delta S^0/R - \Delta H^0/RT \quad (12)$$

where K_α is the thermodynamic equilibrium constant (Equation (13)):

$$K_a = C_s/C_e \quad (13)$$

where C_s and C_e is the solid ($mg \cdot g^{-1}$) and liquid ($mg \cdot L^{-1}$) phase concentration at equilibrium.

4. Conclusions

A hydrothermal treatment was employed to transform spent coffee grounds into AC, previous hydro-alcoholic extraction of the inherent high added value polyphenols. The resulting ACs obtained under different experimental conditions have a microporous structure with specific surfaces greater than 1600 $m^2 \cdot g^{-1}$ that gives them excellent adsorption properties. The adsorption capacity of MB on the AC obtained under optimum conditions has been studied. Moreover, evaluated extracts are characterized by high values of both total flavonoid and total polyphenol content, as well as considerable antioxidant activities. All these results give rise to high-quality products, with potential interest for many industries, can be derived from spent coffee grounds, presenting a real alternative for its most common use, organic fertilizer.

Supplementary Materials: The following are available online, Table S1: Plan of experiments for the two-level factorial design aimed to optimization of polyphenol extraction conditions, Table S2: Plan of experiments for the two-level factorial design for obtaining activated carbon from the solid residue recovered after polyphenol extraction, Table S3: Phenolic compounds extracted from spent coffee grounds, Table S4: Fitted parameter values obtained from the linear mathematical model described in Equation (1) for the extraction of polyphenols, Table S5: Fitted parameter values obtained from the linear mathematical model described in Equation (1) for activated carbon, Table S6: Porosity features of the activated carbons.

Author Contributions: M.E.L. conceptualization, methodology and supervision; S.P.F and N.R.C formal analysis; M.R.G and L.A. formal analysis, investigation, writing original draft and writing-review &editing; F.A.L. conceptualization, methodology, resources, supervision and writing&editing. All authors contributed to the review, edit, and approval of the paper.

Funding: The Comunidad of Madrid and European funding from FSE and FEDER programs for financial support (project S2018/BAA-4393, AVANSECAL-II-CM). We acknowledge support of the publication fee by the CSIC Open Access Publication Support. Initiative through its Unit of Information Resources for Research (URICI).

Acknowledgments: To the Technical Research Support Unit of the Institute of Catalysis and Petroleum Chemistry (CSIC) for support in the textural characterization of activated carbon. Mª Eugenia Léon-González, Noelia Rosales-Conrado and Yolanda Madrid thank the Spanish Commission of Science and Technology (CTQ2017-83569-C2-1-R) and the Comunidad of Madrid and European funding from FSE and FEDER programs for financial support (project S2018/BAA-4393, AVANSECAL-II-CM).

Conflicts of Interest: There are no conflict to declare.

References

1. Birkenberg, A.; Birner, R. The world's first carbon neutral coffee: Lessons on certification and innovation from a pioneer case in Costa Rica. *J. Clean. Prod.* **2018**, *189*, 485–501.
2. Campos-Vega, R.; Loarca-Piña, G.; Vergara-Castañeda, H.A.; Dave Oomah, B. Spent coffee grounds: A review on current research and future prospects. *Trends Food Sci. Technol.* **2015**, *45*, 24–36.
3. Dong, W.; Hu, R.; Chu, Z.; Zhao, J.; Tan, L. Effect of different drying techniques on bioactive components, fatty acid composition, and volatile profile of robusta coffee beans. *Food Chem.* **2017**, *234*, 121–130.
4. Murthy, P.S.; Madhava Naidu, M. Sustainable management of coffee industry by-products and value addition—A review. *Resour. Conserv. Recycl.* **2012**, *66*, 45–58.
5. Ricciardi, P.; Torchia, F.; Belloni, E.; Lascaro, E.; Buratti, C. Environmental characterisation of coffee chaff, a new recycled material for building applications. *Constr. Build. Mater.* **2017**, *147*, 185–193.
6. Suganya, S.; P., S.K. Influence of ultrasonic waves on preparation of active carbon from coffee waste for the reclamation of effluents containing Cr(VI) ions. *J. Ind. Eng. Chem.* **2018**, *60*, 418–430.
7. Iriondo-DeHond, A.; Aparicio García, N.; Velazquez Escobar, F.; San Andres, M.I.; Sanchez-Fortun, S.; Blanch, G.P.; Fernandez-Gomez, B.; Guisantes Batan, E.; del Castillo, M.D. Validation of coffee by-products as novel food ingredients. *Innov. Food Sci. Emerg. Technol.* **2018**, 0–1.
8. Janissen, B.; Huynh, T. Chemical composition and value-adding applications of coffee industry by-products: A review. *Resour. Conserv. Recycl.* **2018**, *128*, 110–117.
9. Franciski, M.A.; Peres, E.C.; Godinho, M.; Perondi, D.; Foletto, E.L.; Collazzo, G.C.; Dotto, G.L. Development of CO_2 activated biochar from solid wastes of a beer industry and its application for methylene blue adsorption. *Waste Manag.* **2018**, *78*, 630–638.
10. Du, C.; Abdullah, J.J.; Greetham, D.; Fu, D.; Yu, M.; Ren, L.; Li, S.; Lu, D. Valorization of food waste into biofertiliser and its field application. *J. Clean. Prod.* **2018**, *187*, 273–284.
11. Kovalcik, A.; Obruca, S.; Marova, I. Valorization of Spent Coffee Grounds: A review. *Food Bioprod. Process.* **2018**, *110*, 104–119.
12. Vijayalaxmi, S.; Jayalakshmi, S.K.; Sreeramulu, K. Polyphenols from different agricultural residues: extraction, identification and their antioxidant properties. *J. Food Sci. Technol.* **2015**, *52*, 2761–2769.
13. Engida, A.M.; Faika, S.; Nguyen-Thi, B.T.; Ju, Y.H. Analysis of major antioxidants from extracts of Myrmecodia pendans by UV/visible spectrophotometer, liquid chromatography/tandem mass spectrometry, and high-performance liquid chromatography/UV techniques. *J. Food Drug Anal.* **2015**, *23*, 303–309.
14. Deshmukh, R.; Kaundal, M.; Bansal, V.; Samardeep Caffeic acid attenuates oxidative stress, learning and memory deficit in intra-cerebroventricular streptozotocin induced experimental dementia in rats. *Biomed. Pharmacother.* **2016**, *81*, 56–62.
15. García-Blanco, T.; Dávalos, A.; Visioli, F. Tea, cocoa, coffee, and affective disorders: vicious or virtuous cycle? *J. Affect. Disord.* **2017**, *224*, 61–68.
16. Castro, A.C.C.M.; Oda, F.B.; Almeida-Cincotto, M.G.J.; Davanço, M.G.; Chiari-Andréo, B.G.; Cicarelli, R.M.B.; Peccinini, R.G.; Zocolo, G.J.; Ribeiro, P.R.V.; Corrêa, M.A.; et al. Green coffee seed residue: A sustainable source of antioxidant compounds. *Food Chem.* **2018**, *246*, 48–57.
17. Rui, L.; Xie, M.; Hu, B.; Zhou, L.; Saeeduddin, M.; Zeng, X. Enhanced solubility and antioxidant activity of chlorogenic acid-chitosan conjugates due to the conjugation of chitosan with chlorogenic acid. *Carbohydr. Polym.* **2017**, *170*, 206–216.
18. S., S.; P., S.K. Influence of ultrasonic waves on preparation of active carbon from coffee waste for the reclamation of effluents containing Cr(VI) ions. *J. Ind. Eng. Chem.* **2018**, *60*, 418–430.
19. Amerkhanova, S.; Shlyapov, R.; Uali, A. The active carbons modified by industrial wastes in process of sorption concentration of toxic organic compounds and heavy metals ions. *Colloids Surfaces A Physicochem. Eng. Asp.* **2017**, *532*, 36–40.
20. Rattanapan, S.; Srikram, J.; Kongsune, P. Adsorption of Methyl Orange on Coffee grounds Activated Carbon. *Energy Procedia* **2017**, *138*, 949–954.
21. Alcaraz, L.; López Fernández, A.; García-Díaz, I.; López, F.A. Preparation and characterization of activated carbons from winemaking wastes and their adsorption of methylene blue. *Adsorpt. Sci. Technol.* **2018**, *36*, 1331–1351.
22. Laksaci, H.; Khelifi, A.; Trari, M.; Addoun, A. Synthesis and characterization of microporous activated carbon from coffee grounds using potassium hydroxides. *J. Clean. Prod.* **2017**, *147*, 254–262.
23. Alguacil, F.; Alcaraz, L.; García-Díaz, I.; López, F. Removal of Pb2+ in Wastewater via Adsorption onto an Activated Carbon Produced from Winemaking Waste. *Metals (Basel).* **2018**, *8*, 697.
24. Ibupoto, A.S.; Qureshi, U.A.; Ahmed, F.; Khatri, Z.; Khatri, M.; Maqsood, M.; Brohi, R.Z.; Kim, I.S.

Reusable carbon nanofibers for efficient removal of methylene blue from aqueous solution. *Chem. Eng. Res. Des.* **2018**, *136*, 744–752.

25. Pawar, R.R.; Lalhmunsiama; Gupta, P.; Sawant, S.Y.; Shahmoradi, B.; Lee, S.M. Porous synthetic hectorite clay-alginate composite beads for effective adsorption of methylene blue dye from aqueous solution. *Int. J. Biol. Macromol.* **2018**, *114*, 1315–1324.
26. Altintig, E.; Kirkil, S. Preparation and properties of Ag-coated activated carbon nanocomposites produced from wild chestnut shell by ZnCl2 activation. *J. Taiwan Inst. Chem. Eng.* **2016**, *63*, 180–188.
27. Filippín, A.J.; Luna, N.S.; Pozzi, M.T.; Pérez, J.D. Obtención Y Caracterización De Carbón Activado a Partir De Residuos Olivícolas Y Oleícolas Por Activacion Física Obtaining and Characterizing of Carbon Activated From Olivic and Olive-Residues By Physical Activation. **2017**, *8*, 59–71.
28. Cheng, S.; Zhang, L.; Ma, A.; Xia, H.; Peng, J.; Li, C.; Shu, J. Comparison of activated carbon and iron/cerium modified activated carbon to remove methylene blue from wastewater. *J. Environ. Sci. (China)* **2016**.
29. Alcaraz, L.; López Fernández, A.; García-Díaz, I.; López, F.A. Preparation and characterization of activated carbons from winemaking wastes and their adsorption of methylene blue. *Adsorpt. Sci. Technol.* **2018**, *36*, 1331–1351.
30. Senthil Kumar, P.; Fernando, P.S.A.; Ahmed, R.T.; Srinath, R.; Priyadharshini, M.; Vignesh, A.M.; Thanjiappan, A. Effect of Temperature on the Adsorption of Methylene Blue dye onto Sulfuric acid-treated orange peel. *Chem. Eng. Commun.* **2014**, *201*, 1526–1547.
31. Hall, K.R.; Eagleton, L.C.; Acrivos, A.; Vermeulen, T. Pore- and Solid-Diffusion Kinetics in Fixed-Bed Adsorption under Constant-Pattern Conditions. *Ind. Eng. Chem. Fundam.* **1966**, *5*, 212–223.
32. Boparai, H.K.; Joseph, M.; O'Carroll, D.M. Kinetics and thermodynamics of cadmium ion removal by adsorption onto nano zerovalent iron particles. *J. Hazard. Mater.* **2011**, *186*, 458–465.
33. Hassan, A.F.; Elhadidy, H. Production of activated carbons from waste carpets and its application in methylene blue adsorption: Kinetic and thermodynamic studies. *J. Environ. Chem. Eng.* **2017**, *5*, 955–963.
34. Ahmed, M.J.; Dhedan, S.K. Equilibrium isotherms and kinetics modeling of methylene blue adsorption on agricultural wastes-based activated carbons. *Fluid Phase Equilib.* **2012**, *317*, 9–14.
35. HAMEED, B.; DIN, A.; AHMAD, A. Adsorption of methylene blue onto bamboo-based activated carbon: Kinetics and equilibrium studies. *J. Hazard. Mater.* **2007**, *141*, 819–825.
36. Tan, I.A.W.; Ahmad, A.L.; Hameed, B.H. Adsorption of basic dye on high-surface-area activated carbon prepared from coconut husk: Equilibrium, kinetic and thermodynamic studies. *J. Hazard. Mater.* **2008**, *154*, 337–346.
37. Altenor, S.; Carene, B.; Emmanuel, E.; Lambert, J.; Ehrhardt, J.J.; Gaspard, S. Adsorption studies of methylene blue and phenol onto vetiver roots activated carbon prepared by chemical activation. *J. Hazard. Mater.* **2009**, *165*, 1029–1039.
38. Bedin, K.C.; Martins, A.C.; Cazetta, A.L.; Pezoti, O.; Almeida, V.C. KOH-activated carbon prepared from sucrose spherical carbon: Adsorption equilibrium, kinetic and thermodynamic studies for Methylene Blue removal. *Chem. Eng. J.* **2016**, *286*, 476–484.
39. Unur, E. Functional nanoporous carbons from hydrothermally treated biomass for environmental purification. *Microporous Mesoporous Mater.* **2013**, *168*, 92–101.
40. Dural, M.U.; Cavas, L.; Papageorgiou, S.K.; Katsaros, F.K. Methylene blue adsorption on activated carbon prepared from Posidonia oceanica (L.) dead leaves: Kinetics and equilibrium studies. *Chem. Eng. J.* **2011**, *168*, 77–85.
41. Köseoğlu, E.; Akmil-Başar, C. Preparation, structural evaluation and adsorptive properties of activated carbon from agricultural waste biomass. *Adv. Powder Technol.* **2015**, *26*, 811–818.
42. Álvarez-Torrellas, S.; García-Lovera, R.; Rodríguez, A.; García, J. Removal of methylene blue by adsorption on mesoporous carbon from peach stones; 2015; Vol. 43; ISBN 9788895608341.
43. Sayğili, H.; Güzel, F.; Önal, Y. Conversion of grape industrial processing waste to activated carbon sorbent and its performance in cationic and anionic dyes adsorption. *J. Clean. Prod.* **2015**, *93*, 84–93.
44. Auta, M.; Hameed, B.H. Optimized waste tea activated carbon for adsorption of Methylene Blue and Acid Blue 29 dyes using response surface methodology. *Chem. Eng. J.* **2011**, *175*, 233–243.
45. Aldawsari, A.; Ali Khan, M.; Hameed, B.H.; AlOthman, Z.A.; Raza Siddiqui, M.; Hadj Ahmed, A.Y.B.; Alsohaimi, I.H. Development of activated carbon from Phoenix dactylifera fruit pits: Process optimization, characterization, and methylene blue adsorption; 2017; Vol. 62;.
46. León-González, M.E.; Gómez-Mejía, E.; Rosales-Conrado, N.; Madrid-Albarrán, Y. Residual brewing yeast as a source of polyphenols: Extraction, identification and quantification by chromatographic and chemometric tools. *Food Chem.* **2018**, *267*, 246–254.
47. Shrikanta, A.; Kumar, A.; Govindaswamy, V. Resveratrol content and antioxidant properties of underutilized fruits. *J. Food Sci. Technol.* **2015**, *52*, 383–390.

48. Langmuir, I. The Adsorption of gases on plane surfaces of glass, mica and platinum. *J. Am. Chem. Soc.* **1918**, *40*, 1361–1403.
49. Freundlich, H.; Heller, W. The Adsorption of cis - and trans -Azobenzene. *J. Am. Chem. Soc.* **1939**, *61*, 2228–2230.
50. Johnson, R.D.; Arnold, F.H. The temkin isotherm describes heterogeneous protein adsorption. *Biochim. Biophys. Acta (BBA)/Protein Struct. Mol.* **1995**, *1247*, 293–297.
51. Adebisi, G.A.; Chowdhury, Z.Z.; Alaba, P.A. Equilibrium, kinetic, and thermodynamic studies of lead ion and zinc ion adsorption from aqueous solution onto activated carbon prepared from palm oil mill effluent. *J. Clean. Prod.* **2017**, *148*, 958–968.
52. Ho, Y..; McKay, G. Pseudo second order model for sorption processes. *Process Biochem.* **1999**, *34*, 451–465.
53. El-Aila, H.J.; Elsousy, K.M.; Hartany, K.A. Kinetics, equilibrium, and isotherm of the adsorption of cyanide by MDFSD. *Arab. J. Chem.* **2016**, *9*, S198--S203.